



Imaging of intracranial haemorrhage

Chelsea S Kidwell, Max Wintermark

Lancet Neurol 2008; 7: 256–67

Department of Neurology and Stroke Center, Georgetown University and Stroke Center, Washington Hospital Center, Washington DC, USA (C S Kidwell MD); and Department of Radiology, University of California San Francisco, San Francisco, CA, USA (M Wintermark MD)

Correspondence to: Chelsea S Kidwell, 110 Irving Street NW, East Building Room 6126, Washington, DC 20010, USA
ck256@georgetown.edu

Intracranial haemorrhage can be a devastating disorder that requires rapid diagnosis and management. Neuroimaging studies are not only required for diagnosis but also provide important insights into the type of haemorrhage, the underlying aetiology, and the accompanying pathophysiology. Historically, CT has been the diagnostic imaging study of choice; however, there is a growing body of data that suggest that MRI is at least as sensitive as CT to detect haemorrhage in the hyperacute setting, and superior to CT in the subacute and chronic settings. Blood has characteristic appearances on both imaging modalities at each stage (acute, subacute, and chronic) and it is important that physicians are familiar with the appearance of various types of intracranial haemorrhage on CT and MRI and their clinical implications. In addition, new imaging applications, such as magnetic resonance spectroscopy and diffusion tensor imaging, are promising research techniques that have the potential to enhance our understanding of the tissue injury and recovery that result from intracranial haemorrhage.

Introduction

Intracranial haemorrhage is a devastating disorder that has poor prognoses and high mortality rates.¹ Advances in neuroimaging techniques have improved our diagnostic capabilities, increased our understanding of the underlying pathophysiology and aetiology of intracranial haemorrhage, and helped to establish prognoses. For example, rapid multimodal CT and MRI can now be done in real-time in the acute clinical setting, which enables prompt diagnosis of haemorrhage on parenchymal imaging and can also show vessel malformations and other underlying structural lesions on additional sequences. In particular, the introduction of blood-sensitive gradient echo sequences has enabled MRI to become a clinically useful technique to detect acute haemorrhage. A classification of the major types of adult intracranial haemorrhage is provided (panel 1).

First, we review the neuroimaging characteristics and development of signal change in response to blood breakdown products seen on CT and MRI at various stages. Then, the appearance of haemorrhage on CT and MRI sequences will be reviewed by individual haemorrhage types (intraparenchymal haemorrhage, subarachnoid haemorrhage, subdural haematoma, and epidural haematoma), with a discussion of the relevant clinical implications. Finally, we discuss other promising research techniques and their relevance. The reader is referred to other publications for more detailed discussions of the epidemiology, clinical characteristics, and management of these disorders.^{2,3}

Physical principles

A basic knowledge of the pathophysiology and development of intracranial haemorrhage is essential to understand the sequential imaging changes seen on CT and MRI. Intracranial haemorrhages are typically divided into five distinct stages on the basis of blood breakdown products (table and webfigure 1): hyperacute (<12 h); acute (12 h to 2 days); early subacute (2–7 days); late subacute (8 days to 1 month); and chronic (>1 month to years).

In the hyperacute stage, the intracranial haemorrhage is a liquid composed of 99% intracellular oxygenated haemoglobin. During the next few hours, a heterogeneous clot develops that comprises blood cells, platelets, and protein-rich serum. As the clot retracts, the expelled serum and the reactive vasogenic oedema in the adjacent brain parenchyma surround it. During the acute stage, the intracellular haemoglobin is progressively deoxygenated, and in the subsequent early subacute phase, there is oxidative denaturation of haemoglobin, and deoxyhaemoglobin is gradually converted to methaemoglobin. During the late subacute stage, lysis of the red blood cells results in the release of methaemoglobin into the extracellular space, and the surrounding vasogenic oedema slowly subsides. During the chronic stage, macrophages and astroglial cells surround and slowly phagocytise the haematoma. Extracellular methaemoglobin is stored in the macrophages and is converted into haemosiderin and ferritin. Eventually, the haematoma will resolve completely, leaving a fluid-filled cyst or collapsed brain defect as a sequelae.⁴ Time-dependent changes in intracranial haemorrhage are influenced by local alterations in haematocrit, pH, and oxygen tension.

The CT imaging characteristics of intracranial haemorrhage are determined by the degree that the X-rays are attenuated by the blood products. The haematocrit, degree of blood clot retraction, and haemoglobin content determine the density of the lesion seen on CT.⁴ The appearance of an intracranial haemorrhage on CT parallels the temporal evolution of the haemorrhage. In the hyperacute and acute phases the clot is hyperdense compared with the adjacent healthy brain parenchyma. During the first few hours post-haemorrhage, the progressive retraction of the clot and extrusion of the serum increases the concentration of haemoglobin, and the density of the haematoma increases; in patients with severe anaemia, reduced concentrations of haemoglobin result in the acute haematoma being less hyperdense than expected. During the late subacute phase, progressive lysis of the

See Online for webfigure 1

red blood cells and proteolysis of the haemoglobin result in decreasing CT density of the haemorrhage, which becomes isodense to the adjacent brain parenchyma. In the chronic phase, the hypodense haematoma is progressively resorbed and typically leaves a small hypodense brain defect.^{4,5}

The magnetic resonance signal characteristics of intracranial haemorrhage are determined by the paramagnetic effects of the breakdown products of haemoglobin, the magnetic field strength, and the pulse sequence used (table).⁵ The breakdown products of haemoglobin are characterised by the different oxidation states of iron and, as such, have different magnetic properties. In the hyperacute stage, because oxygenated haemoglobin has no unpaired electrons and is diamagnetic, the haematoma is isointense or mildly hyperintense on T1-weighted MRI and hyperintense on T2-weighted MRI, owing to the haemoglobin content. Deoxyhaemoglobin has few unpaired electrons and is paramagnetic; consequently, in the acute stage the haemorrhage is isointense or hypointense on T1-weighted MRI and hypointense on T2-weighted MRI. In the early subacute phase, methaemoglobin is paramagnetic and confined to the intracellular compartment, with a magnetic gradient between the intracellular and the extracellular compartments; the haemorrhage is hyperintense on T1-weighted MRI and hypointense on T2-weighted MRI. In the late subacute stage, methaemoglobin is released by lysis of the red blood cells, which cancels the magnetic gradient between the intracellular and the extracellular compartments; the haemorrhage is hyperintense on T1-weighted and T2-weighted MRI. Finally, in the chronic phase, because haemosiderin has many unpaired electrons and is superparamagnetic, the haemorrhage is hypointense on T1-weighted and T2-weighted MRI.^{4,5} Fluid-attenuated inversion recovery (FLAIR) MRI intensity changes for intraparenchymal haemorrhages are the same as those for other T2-weighted MRI sequences.

Until the development of T2*-weighted gradient echo (GRE) MRI sequences, T1-weighted and T2-weighted MRI sequences were used to estimate the age of an intracranial haemorrhage. In the 1990s, it was shown that GRE sequences are highly sensitive to the susceptibility effects of the paramagnetic and superparamagnetic breakdown products of haemoglobin;⁶⁻⁸ this increases the number of haemorrhagic lesions that can be identified.⁹⁻¹¹ Echo-planar T2*-weighted imaging can be done with acquisition times in the seconds, which is a substantial advantage in patients with acute intracranial haemorrhage, who are unable to cooperate; conventional spin-echo images of such patients are often degraded by motion artifacts. The appearance of blood on GRE MRI can also be described by stage. The hallmark of hyperacute haemorrhage on GRE MRI sequences is a

Panel 1: Subtypes of intracranial haemorrhages

Intracerebral haemorrhage

- Primary
 - Haematomas
 - Microbleeds
- Secondary
 - Tumours
 - Vascular malformations
 - Aneurysms
 - Coagulopathy
 - Haemorrhagic transformation of ischaemic stroke
 - Infections
 - Cerebral venous or sinus occlusion
 - Trauma
 - Drug use (eg, sympathomimetics)

Subarachnoid haemorrhage

- Aneurysmal
- Non-aneurysmal

Subdural haematoma

Epidural haematoma

rim of hypointense signal that surrounds an isointense core. In the acute and subacute stages, the haematoma becomes diffusely hypointense, whereas in the chronic stage it appears as a slit-like signal with a hyperintense or isointense core that has a rim of hypointensity. In some cases (eg, small haemorrhages in which the blood becomes rapidly deoxygenated and, therefore, the haemorrhage quickly appears hypointense throughout), GRE MRI sequences cannot help to estimate accurately the age of the haematomas.¹²

The value of diffusion-weighted imaging in the evaluation of intracranial haemorrhage is still under investigation.^{10,11,13,14} Diffusion-weighted imaging has promise in the differentiation of primary intracerebral haemorrhage from haemorrhagic cerebral ischaemia.¹³

Intraparenchymal haemorrhage

Primary (spontaneous) intracerebral haemorrhage

The most common risk factors associated with adult primary intracerebral haemorrhage are hypertension and cerebral amyloid angiopathy, and the probable underlying pathophysiology varies by haemorrhage location.¹⁵ Primary intracerebral haemorrhage associated with hypertension most commonly occurs in deep brain structures (eg, putamen, thalamus, cerebellum, and pons). By contrast, primary intracerebral haemorrhages that occur in lobar regions, particularly in elderly patients, are most commonly related to cerebral amyloid angiopathy but might also be associated with hypertension.¹⁶

Until recently, non-contrast CT was the gold standard for the diagnosis of intracerebral haemorrhage, and at many centres it is still the imaging modality of choice

	CT	T1-weighted MRI	T2-weighted MRI	MRI FLAIR	GRE MRI
Hyperacute (<12 h)	Hyperdense	Isointense or mildly hyperintense	Hyperintense	Hyperintense	Hypointense rim
Acute (12 h to 2 d)	Hyperdense	Isointense or hypointense	Hypointense	Hypointense	Hypointense rim that gradually progresses to centre
Early subacute (2–7 d)	Hyperdense	Hyperintense	Hypointense	Hypointense	Hypointense
Late subacute (8 d to 1 m)	Isodense	Hyperintense	Hyperintense	Hyperintense	Hypointense
Chronic (>1 m)	Hypodense	Isointense or hypointense	Hypointense	Hypointense	Slit-like hyperintense or isointense core that is surrounded by a hypointense rim

Table: Appearance of blood on CT and MRI by stage

for the assessment of intracerebral haemorrhage, owing to its widespread availability and rapid acquisition time. Conventional T1-weighted and T2-weighted MRI pulse sequences are not sensitive to blood in the hyperacute stage; however, several recent studies have now shown that GRE MRI sequences are as accurate as CT for the detection of intraparenchymal haemorrhage and far superior to CT for the detection of chronic haemorrhage (figure 1 and webfigures 2, 3, and 4).^{12,17,18} In some cases, MRI might actually detect haemorrhages that are missed on CT,^{12,19} and MRI is better than CT at identifying underlying structural lesions and for quantifying perihematoma oedema. However, up to 20% of patients with acute stroke are unsuitable for MRI (eg, they have pacemakers or metal implants or are unable to lie flat or still for the duration of the scan).²⁰

For both MRI and CT, baseline and serial studies can be used to identify patients who might benefit from acute interventions (eg, hydrocephalus that requires cerebrospinal fluid drainage or large or expanding cerebellar haematomas that require posterior fossa decompression). Both modalities can include postcontrast studies and vessel angiography to rule out underlying structural lesions (eg, arteriovenous malformation, aneurysm, or tumour). In general, contrast studies and catheter angiography are indicated in patients without a clear underlying aetiology or in patients with haemorrhages in unusual locations.² One recent study suggested a high yield for angiography, even in patients with putaminal haemorrhage, unless the patient is older than 55 years and has hypertension.²¹

Neuroimaging provides considerable information with regard to prognosis. Early CT studies in patients with intracerebral haemorrhage have shown that more than a third of patients have substantial (>33%) haematoma growth when imaged within 3 hours of onset.²² Haematoma expansion is associated with larger baseline haematoma volumes.^{22,23} In turn, haematoma

expansion and the presence of intraventricular haemorrhage (webfigure 5) are predictors of poor outcome. Cortical intracerebral haemorrhage can be associated with better functional outcome; however, the rate of long-term recurrence is increased by a factor of 3·8.^{1,24} Several recent studies have reported that contrast extravasation seen on CT angiography might also be an early predictor of haematoma expansion (figure 2)^{25,26} and poor outcome.²⁷ Therefore, CT angiography could have important applications for the selection of patients for acute therapies (eg, blood pressure management or haemostatic therapy).

Imaging techniques also provide insights into the underlying pathophysiology of intracerebral haemorrhage. Interest in these imaging approaches is driven by the belief that poor outcome in primary intracerebral haemorrhage results, in part, from ongoing secondary neuronal injury in the perihematoma region. Some of the studies that use PET, single-photon emission computed tomography (SPECT), and, more recently, perfusion MR and perfusion CT have shown perihematoma regions of hypoperfusion and bioenergetic compromise.^{28–35} The results of MRI studies have suggested that approximately a third of patients who are imaged in the acute phase will have reduced perihematoma apparent diffusion coefficient abnormalities on diffusion-weighted imaging, and further studies have characterised the timecourse for early perihematoma changes.^{32,36,37} Apparent diffusion coefficient values were low during the first day and then gradually increased, which probably matches the development of perihematoma oedema.

Alternatively, the results of studies with various imaging modalities have suggested that frank perihematoma hypoperfusion that reaches classic ischaemic thresholds does not occur.^{29,38–40} Specifically, the results of PET studies have not shown evidence of hypoxia or ischaemia (ie, normal oxygen extraction fraction and ¹⁸F-fluoromisonidazole uptake) surrounding intracerebral haemorrhage; therefore, the most prevalent hypothesis to account for perihematoma hypoperfusion is that it is due to secondary metabolic disturbances. The timecourse of these changes might explain the conflicting findings among studies.⁴¹ Analysis of the studies performed to date shows that there might be a subset of patients with a rim of perihematoma hypoperfusion and possibly ischaemia in the hyperacute phase; however, this region rapidly disappears in the subacute phase as oedema and inflammation develop.^{34,35} The development of oedema and toxicity from blood breakdown products are the most significant contributors to ongoing perihematoma injury, and imaging studies have the potential to monitor the effect on recovery and the influences of putative interventions on these parameters.^{28,42}

See Online for webfigures 2, 3, 4, and 5

Microbleeds

GRE MRI has the ability to not only detect acute and chronic haematomas but also old, clinically silent cerebral microbleeds that are not seen on CT. Microbleeds are generally defined as punctate, homogeneous, rounded, hypointense lesions in the parenchyma that are smaller than 5–10 mm (figure 1 and webfigures 2 and 4). Pathological studies have shown that microbleeds seen with GRE MRI usually correspond to haemosiderin-laden macrophages adjacent to small vessels and are indicative of previous extravasation of blood.⁴³

Microbleeds have been seen in up to 80% of patients with primary intracerebral haemorrhage, 21–26% of patients with ischaemic stroke, and 5–6% of asymptomatic or healthy elderly individuals.^{43–50} Hypertension, cerebral amyloid angiopathy, getting older, and, less commonly, cerebral autosomal dominant arteriopathy with silent infarcts and leukoencephalopathy (CADASIL) have been identified as important risk factors for microbleeds.^{49,51–53} Recently, a mutation in *COL4A1*, the gene that encodes the basement membrane protein procollagen type IV alpha 1, has been reported in a French family; this mutation leads to small vessel cerebral disease, intracerebral haemorrhage, and microbleeds.^{54,55}

Microbleeds have been suggested to be markers of a bleeding-prone angiopathy.^{56–58} The results of several case reports and small series suggest that patients with microbleeds might be at increased risk of haemorrhage after antithrombotic or thrombolytic therapies. By contrast, the results of two large studies did not show an increased risk of haemorrhage in patients with microbleeds who were treated with intravenous tissue plasminogen activator.^{59,60} However, in both studies, few patients with large microbleed burdens were included and, therefore, the risk of haemorrhage in patients with a large number of microbleeds (>5) is unknown.

Microbleeds have important prognostic significance and are a common occurrence in patients with cerebral amyloid angiopathy; they are most commonly found in lobar regions (figure 1).⁵¹ By contrast, in patients with intracerebral haemorrhage due to hypertensive disease, microbleeds are most commonly found in deep and infratentorial regions (webfigure 4), although hypertension can also contribute to lobar microbleeds.⁴⁹ A pattern of multiple haemorrhages without an underlying cause and restricted to lobar regions in an elderly patient is highly indicative of a diagnosis of cerebral amyloid angiopathy with the Boston Criteria.⁶¹ A particularly noteworthy finding is that the total number of microbleeds predict the risk of future symptomatic intracerebral haemorrhage in patients with lobar haemorrhage and probable cerebral amyloid angiopathy.⁶² Moreover, in this population, new microbleeds seen on repeat MRI also predict increased risk of subsequent symptomatic intracerebral

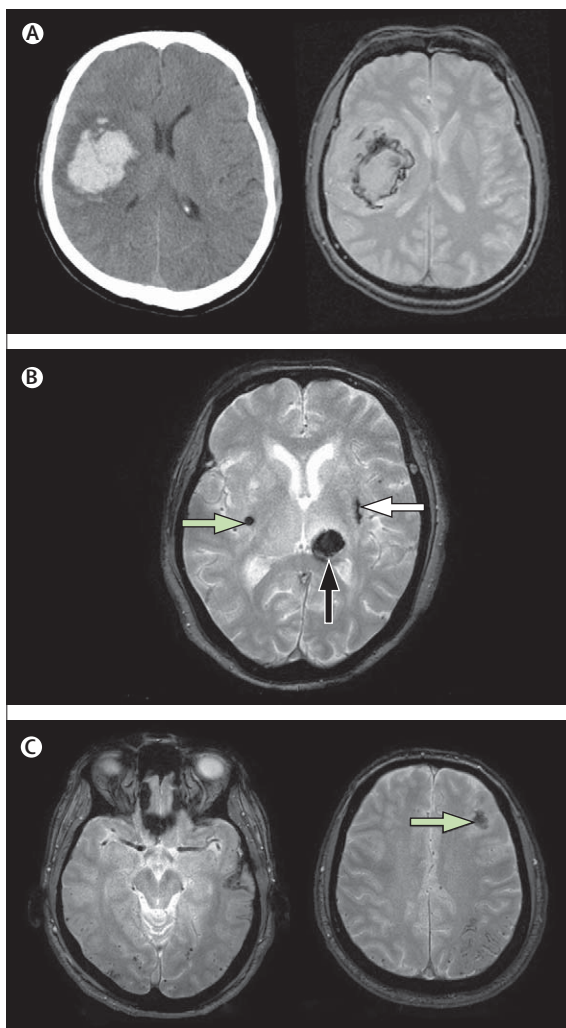


Figure 1: Examples of primary intracerebral haemorrhage

(A) Appearance of acute hypertensive haemorrhage on CT (left) and GRE MRI (right) both obtained within 12 h of symptom onset. GRE MRI shows a classic rim of hypointense signal surrounding the core of the haematoma. (B) Subacute left thalamic intracerebral haemorrhage (black arrow), chronic haematoma with slit-like appearance (white arrow), and large microbleed (green arrow), all seen with GRE MRI. (C) GRE MRI that shows a large number of lobar microbleeds in the setting of an acute left frontal intracerebral haemorrhage. These are consistent with underlying cerebral amyloid angiopathy. A larger version of (C) can be found online (webfigure 2).

haemorrhage, and microbleed burden and the rate of their accumulation predicts cognitive decline and poor neurological or functional outcome.⁶² The presence and lesion burden of microbleeds are notable prognostic factors in hypertensive haemorrhage. Several studies have shown a correlation between microbleeds and new vascular events.^{52,63}

Secondary intracerebral haemorrhage

Intracerebral haemorrhage can be secondary to a large number of underlying pathologies (panel 1), many of which have distinct imaging characteristics. Multimodal

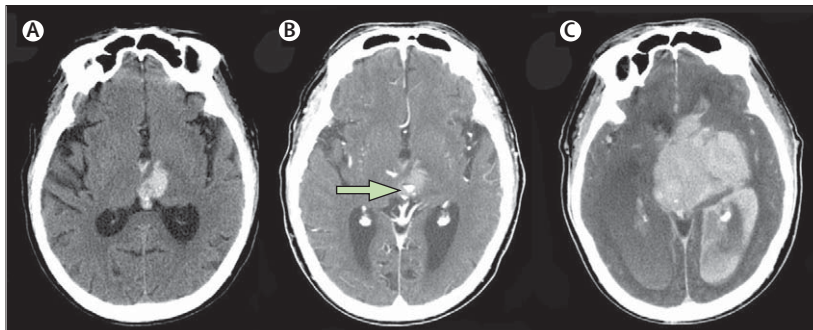


Figure 2: Imaging of a 69-year-old man 2 hours after the onset of right-sided paralysis
 (A) Non-contrast CT taken on admission shows left thalamic haematoma with extension of the haemorrhage into the third ventricle. (B) Contrast-enhanced CT taken on admission shows active extravasation within the haematoma. (C) Follow-up non-contrast CT taken 12 hours after admission shows notable growth of the haematoma, with haemorrhage in both lateral ventricles and severe hydrocephalus. Active contrast extravasation in intraparenchymal haematoma as seen with CT angiography and postcontrast CT predicts mortality and haematoma growth.²⁷

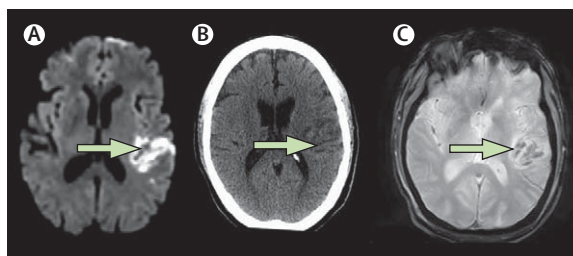


Figure 3: Example of haemorrhagic transformation of an infarct in a branch of the left middle cerebral artery
 The infarct is seen with (A) diffusion-weighted imaging, (B) CT, and (C) GRE MRI.

MRI or CT can help to identify the underlying pathology, although in some cases this might be obscured by the acute haematoma.

Underlying vascular lesions are more common in patients with intracerebral haemorrhages located in lobar lesions, and larger haematomas are more commonly associated with arteriovenous malformations. With an underlying arteriovenous malformation, flow voids can be seen, particularly on MRI. CT angiography or MR angiography might reveal the underlying vascular lesion; however, in some cases, catheter angiography is required and might need to be repeated if the results were initially negative owing to the mass effect of the haematoma. The findings from imaging that might be deemed indications for catheter angiography include abnormal calcifications, the presence of subarachnoid blood, vessel abnormalities, or unusual haemorrhage locations.² Cavernous malformations are best seen on GRE MRI sequences and appear as a hypointense ring (due to haemosiderin from a previous bleeding event) around the malformation (webfigure 3). Isolated cavernomas can be difficult to diagnose in the acute phase because their appearance can resemble that of a primary haemorrhage.

Imaging can also provide clues to non-vascular aetiologies of intracerebral haemorrhage. Traumatic intracerebral haemorrhage is commonly accompanied

Panel 2: CT classification of haemorrhagic transformation

Haemorrhagic infarction type 1 (HI-1)

Small petechiae along the margins of the infarct

Haemorrhagic infarction type 2 (HI-2)

More confluent petechiae within the infarcted area but without space-occupying effect

Parenchymal haematoma type 1 (PH-1)

Haematoma in up to 30% of infarcted area with some space-occupying effect

Parenchymal haematoma type 2 (PH-2)

Dense haematoma in more than 30% of infarcted area with substantial space-occupying effect or any haemorrhagic lesion outside the infarcted area

by evidence of a scalp haematoma and a coup–contrecoup location. Contusions have a marked predilection for the orbitofrontal regions and the anterior temporal lobes. The presence of a fluid–blood level (ie, the horizontal interface between hypodense bloody serum layered above hyperdense settled blood) is highly suggestive of a traumatic aetiology or an underlying coagulopathy.^{64,65} In one study, the presence of a fluid–blood level had 59% sensitivity and 98% specificity for abnormal prothrombin time or partial thromboplastin time (ie, the time it takes for the blood to clot).⁶⁵ Haemorrhagic lesions associated with diffuse axonal injury from traumatic shearing lesions can be seen on MRI, particularly with high-spatial-resolution, susceptibility-weighted techniques.⁶⁶

Haemorrhages due to sinus occlusions are typically found in the parasagittal region if the thrombosis is superficial, or they are bithalamic if due to occlusion of the deep sinuses. An underlying vascular lesion (aneurysm or arteriovenous malformation)⁶⁷ or a vasculopathic pattern on invasive or non-invasive vessel imaging studies can be seen in intracerebral haemorrhages that accompany drug use. Tumours are typically enhanced on postcontrast studies and have been shown to have substantially greater amounts of vasogenic oedema compared with intracerebral haemorrhages due to other aetiologies.⁶⁸ Haemorrhages due to underlying infections commonly have lesion enhancement.

Haemorrhagic transformation

Haemorrhagic transformation of an ischaemic infarct occurs commonly as part of the natural history of the disease and in the setting of reperfusion therapies. The most commonly used radiological classification system for rating the type and severity of haemorrhagic transformation on head CT scans divides the haemorrhage into two major categories: haemorrhagic infarct (figure 3) and parenchymal haematoma (webfigure 6); each division is subdivided into two subcategories on the basis of severity (panel 2).⁶⁹

See Online for webfigure 6

The application of this classification system to MRI has not been systematically assessed and compared with CT. Moreover, studies have shown that GRE MRI sequences are more sensitive to haemorrhagic transformation than is CT (figure 3), which makes the standard classification across modalities problematic.⁷⁰ In one study of 25 patients, GRE MRI sequences detected haemorrhagic transformation in 12 patients compared with 7 patients detected with CT.⁷¹

Imaging information can help to distinguish the haemorrhagic transformation of an ischaemic infarct from a primary haematoma. Most haemorrhagic transformations are smaller than the field of the ischaemic infarct. Thus, FLAIR MRI sequences, diffusion-weighted imaging, and the apparent diffusion coefficient sequence can provide information from the non-haemorrhagic regions and show that the blood is within a larger ischaemic infarct. Primary haematomas also tend to be rounder and commonly have a greater amount of surrounding oedema than would be seen in an ischaemic stroke. Furthermore, haematomas do not necessarily respect vascular territories.

A growing number of studies have assessed the clinical and radiological predictors of haemorrhagic transformation in the setting of thrombolytic therapy. In the NINDS trial⁷² of intravenous tissue plasminogen activator given within 3 hours of onset, the presence of signs of early infarct was associated with an increased risk of subsequent haemorrhagic transformation in the treated group; however, this association was not independent of baseline variables, which included the National Institutes of Health Stroke Scale score to measure the neurological deficit, and these patients fared better with tissue plasminogen activator treatment.⁷² In the European Cooperative Acute Stroke Study I (ECASS I), patients enrolled in the trial who had signs of major (involving more than a third of middle cerebral artery territory) early infarct on CT (protocol violators) had an increased rate of haemorrhagic transformation compared with patients without signs of extended early infarct on CT; the patients with signs of major infarct did not benefit from thrombolytic therapy.⁷³ An analysis of the subsequent ECASS II results revealed that the extent of hypoattenuation at baseline was an independent risk factor for severe haemorrhagic transformation.⁷⁴ Thus, on the basis of the results of these trials, CT changes detected within 3 hours that involve more than a third of the middle cerebral artery territory do not constitute a contraindication to tissue plasminogen activator treatment, whereas beyond 3 hours they would. Of note, the results of secondary analyses from these two ECASS studies have suggested that only parenchymal haematoma type 2 (webpanel 2) lesions are associated with clinical deterioration and poor prognosis,^{69,75} although this is controversial.⁷⁶

On both CT and MRI, contrast extravasation is a marker of blood–brain barrier disruption and a predictor

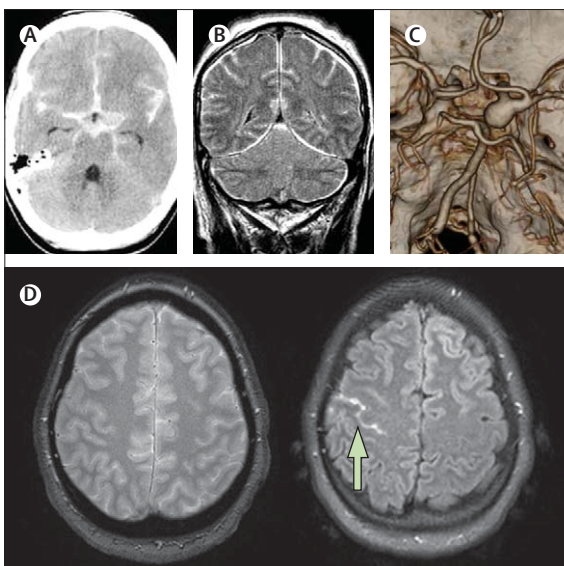


Figure 4: 35-year-old woman who presented with thunderclap headaches (A) Non-contrast CT shows diffuse subarachnoid haemorrhage. (B) Confirmation of subarachnoid haemorrhage with FLAIR MRI. (C) CT angiography, viewed from above, depicts a ruptured aneurysm in the right posterior communicating artery (arrow), which is responsible for the subarachnoid haemorrhage. (D) Example of superficial subarachnoid haemorrhage visualised on FLAIR (arrow) but not GRE MRI sequences.

of haemorrhagic transformation.^{77–79} In addition, a growing number of MRI studies have identified additional imaging characteristics that predict haemorrhagic transformation. The results of several of these studies have suggested that large baseline diffusion-weighted imaging lesions and low apparent diffusion coefficient values are independent predictors of symptomatic haemorrhage.^{80–82} These are important areas for future research and provide a potential biomarker to identify high-risk patients and test therapies designed to minimise the risk of blood–brain barrier opening and subsequent haemorrhagic transformation.

Subarachnoid haemorrhage

Immediately after a subarachnoid haemorrhage, the subarachnoid space is filled with erythrocytes suspended in the CSF. The erythrocytes are trapped within the arachnoid villi and trabeculae and are progressively cleared from the CSF into the vascular system or phagocytically removed by leptomeningeal macrophages while red blood cell lysis releases haemoglobin in the CSF.

Subarachnoid haemorrhage can be of traumatic or non-traumatic origin, with trauma being the most common aetiology. Subarachnoid haemorrhage can occur in head injury, as a result of laceration of the cortical veins or arteries that course through the subarachnoid space but can also occur as a result of cortical contusions and lacerations with extravasation of blood into the

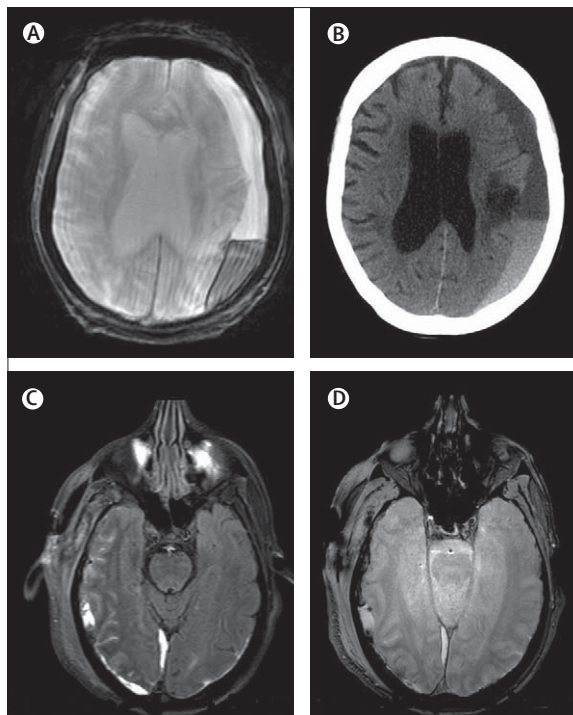


Figure 5: Two examples of subdural haematomas
 (A,B) Extensive left hemisphere subdural haematoma seen on GRE MRI (A) and CT (B). Note blood fluid levels on both studies. (C,D) Traumatic subdural haematomas and subarachnoid blood seen on FLAIR MRI (C) and GRE MRI sequence (D). Acute blood is hyperintense on FLAIR MRI and either hypointense or isointense on GRE MRI. Note the large right scalp contusion.

subarachnoid space. Typical locations for subarachnoid haemorrhage after head trauma are the interpeduncular cistern, Sylvian fissure, or over the cerebral convexity.⁸³ Spontaneous subarachnoid haemorrhage usually results from ruptured aneurysms (older patients), arteriovenous vascular malformations (younger patients), and can be less commonly due to intracranial vessel dissection or vasculitis. Perimesencephalic (or pretruncal) non-aneurysmal subarachnoid haemorrhage is a benign variant of unknown (probably venous) cause, with the centre of bleeding most commonly located in the prepontine cistern. Subarachnoid haemorrhage can also be present in Call–Fleming syndrome—a generally benign and reversible condition due to segmental cerebral vasoconstriction that presents with severe recurrent headaches and transient or fluctuating neurological abnormalities.⁸⁴

CT is sensitive in detecting blood in the CSF space and is usually more easily available than MRI in the acute setting of subarachnoid haemorrhage (figure 4). Typically, in patients with acute subarachnoid haemorrhages, hyperdense blood is seen within the basal cisterns and subarachnoid spaces. In about 10% of cases, the CT will be negative, particularly when obtained more than 12 hours after the onset of symptoms, and a lumbar puncture is required to

confirm the diagnosis. The location and distribution of the subarachnoid haemorrhage can indicate the site of the vascular malformation, and contrast-enhanced CT angiography can show the exact location and shape of the aneurysm.⁸⁵

Acute subarachnoid haemorrhage is difficult to detect with conventional T1-weighted and T2-weighted MRI sequences. Subarachnoid haemorrhage differs from intraparenchymal haemorrhage in that the mixing of blood with high oxygen tension CSF delays the generation of paramagnetic deoxyhaemoglobin, and oxyhaemoglobin persists for longer than in intraparenchymal haemorrhage.^{86,87} Variability in the appearance of subarachnoid haemorrhage after 48 hours most probably relates to haemoglobin degradation, which adds further complexity to the MRI signal intensity.⁸⁸

FLAIR MRI is sensitive enough to detect acute subarachnoid haemorrhage because suppression of the CSF signal enhances the conspicuity of the haemorrhage (webfigure 7).^{89–91} The FLAIR MRI techniques consist of an inversion recovery pulse to null the signal from the CSF and a long echo time to produce a heavily T2-weighted sequence.⁹⁰ When disease occurs within the subarachnoid space, the relaxation time of the CSF is altered, which results in a change in the T1-weighted signal; this change translates into reduced CSF signal nulling and consequent hyperintensity of the CSF or subarachnoid space during the FLAIR MRI sequence. Such findings have been well described in a wide range of pathological conditions, including subarachnoid haemorrhage, meningitis,⁹² and the leptomeningeal spread of malignant disease.⁹³ Other, less common, causes of subarachnoid FLAIR MRI hyperintensity include slow flow downstream from vascular stenosis or occlusion,^{92,94} artifacts caused by supplemental oxygen, and sulcal enhancement following contrast administration when the blood–brain barrier is disrupted.^{78,95,96}

The results of in-vivo and in-vitro studies have suggested that FLAIR imaging (figure 4) is at least as sensitive as CT for the evaluation of acute subarachnoid haemorrhage; however, compared with the findings from lumbar puncture, the findings on FLAIR MRI are not definitive in excluding acute subarachnoid haemorrhage.^{97–99} The FLAIR MRI sequence is particularly useful to image acute subarachnoid haemorrhage in areas where CT might be limited because of beam-hardening artifacts.⁹⁸ Few studies have systematically assessed GRE MRI sequences in patients with subarachnoid haemorrhage¹⁰⁰ or compared the accuracy of the sequences with FLAIR MRI, although one recent study suggested good accuracy for GRE MRI sequences when assessed on a 3-Tesla scanner.¹⁰¹

Subdural haematoma

Subdural haematomas can be diagnosed in the acute, subacute, or chronic stages on the bases of location,

See Online for webfigure 7

severity, and various clinical presentations. They can occur after head trauma, coagulopathy, antithrombotic therapy, or spontaneously. They are most commonly seen along the cerebral convexities, the falx cerebri, and the tentorium cerebelli. If caused by trauma, a scalp haematoma or bone fracture might also be seen.

The appearance of subdural haematomas on CT and MRI depends on the stage and location (figure 5). In the acute stage, subdural haematoma typically appears as a hyperdense crescent along the cerebral convexity, a linear hyperdensity between the hemispheres, or a thin hyperdense layering along the tentorium cerebelli. In the subacute stage, subdural haematomas can be difficult to detect on CT because they become isodense to grey matter and might only be apparent because of the mass effect. Chronic subdural haematomas are hypodense compared with grey matter. Recurrent bleeding into the subdural space can lead to a bilayered or mixed pattern, with blood breakdown products at various stages.

The appearance of subdural haemorrhage on MRI depends not only on the stage of the lesion but also on the sequence used. The development of signal changes might not directly correlate with that of intraparenchymal haematomas.¹⁰² The results of a systematic study that compared signal changes in patients who had intracerebral haemorrhage with patients who had subdural haemorrhage showed that, in the acute stage, the subdural haematoma lesions appear as hyperintense on FLAIR MRI and T2-weighted sequences. On GRE MRI sequences, subdural haematomas can be isointense or hypointense in the acute stage, depending on the stage of blood breakdown products. In the subacute stage, the breakdown products appear hypointense, whereas at chronic timepoints they appear as either isointense or mixed signals, depending on the degree of blood reabsorption.

Epidural haematoma

Epidural haematomas usually occur after acute head traumas, and their clinical presentation might be delayed (eg, with a symptom-free or lucid interval). Arterial epidural haematomas usually result from laceration of branches of the meningeal arteries, whereas venous epidural haematomas result from a tear in the dural venous sinuses. Venous epidural haematomas are more commonly seen in children, and can develop more slowly, with less acute symptoms, than arterial epidural haematomas. Epidural haematomas are located between the skull and the periosteal layer of the dura mater. The tight adherence between the dura mater and the skull prevents extension of an epidural haematoma across skull sutures. Epidural haematomas are typically well defined, biconvex, extra-axial lesions, which can displace the adjacent brain (figure 6). A rapidly enlarging arterial epidural haematoma can result in a substantial midline shift,

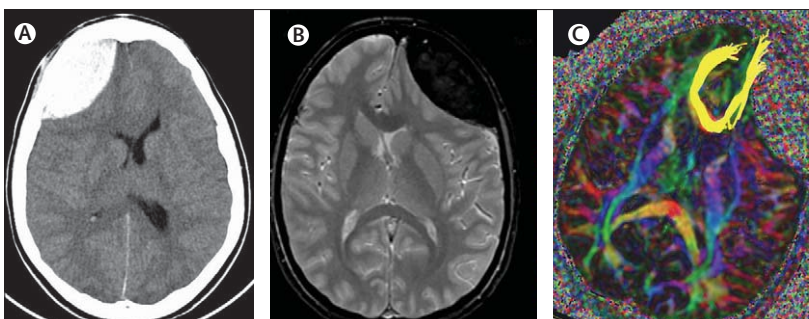


Figure 6: Examples of epidural haematomas

(A) Non-contrast CT of a 20-year-old male patient who was involved in a motor vehicle accident shows a right frontal epidural haematoma, with typical biconvex shape and the non-crossing of sutures. This epidural haematoma resulted from an arterial bleed due to a right frontal calvarial fracture. (B,C) Epidural haematoma that displaced and compressed the white matter tracts of the left frontal lobe in a 22-year-old woman who was imaged 6 days after mild traumatic brain injury (Glasgow coma score of 15). (B) GRE MRI sequence from 3T MRI shows the large lentiform epidural haematoma as a dark signal, space-occupying, extra-axial mass in the left frontal lobe. There is medial displacement and compression of white matter in the left frontal lobe and midline shift to the right, which signifies subfalcine herniation. (C) Directionally encoded colour fractional anisotropy map from 3T diffusion tensor imaging shows white matter tracts with left-right fibre orientation in red, anteroposterior in green, and craniocaudal in blue. 3D fibre tractography of the commissural tracts of the genu of the corpus callosum (bright yellow). Medial deviation of the commissural fibres of the left frontal lobe is evident.

with different degrees of secondary herniation and possible secondary ischaemia.¹⁰³ CT attenuation and MRI signal intensities follow the temporal development of epidural haematomas. No dilution with CSF occurs because an epidural haematoma is separated from the CSF by the dura mater.

New imaging applications

PET and SPECT techniques, although not practical in the acute clinical setting, have provided important information with regard to changes in blood flow and their timecourse, particularly in patients with primary intracerebral haemorrhage. PET imaging with the [¹¹C] Pittsburgh compound-B has been used to detect cerebrovascular β -amyloid in patients with intracerebral haemorrhage that is secondary to amyloid angiopathy.¹⁰⁴

Several additional techniques, including near-infrared spectroscopy, magnetic resonance spectroscopy, and diffusion tensor imaging, promise to provide new insights into the diagnosis and pathophysiology of haemorrhage, the timecourse of cerebral injury, recovery, and neuroplasticity, and the response to putative therapies. Near-infrared spectroscopy shows potential as a diagnostic means for the rapid identification of subdural and epidural haematomas in the field or at the bedside in patients with head trauma.^{105,106}

Several studies have used magnetic resonance spectroscopy to assess perihematoma metabolic and haemodynamic changes in patients with intracerebral haemorrhage. Two small studies have reported metabolic changes in higher cortical structures in patients with deep intracerebral haemorrhage, which suggests that these changes might correlate with long-term motor deficit and clinical outcome.^{107,108}

Search strategy and selection criteria

References were identified through PubMed searches from 1980 to September, 2007, with the search terms "imaging", "intracerebral haemorrhage", "subarachnoid haemorrhage", "microbleeds", "subdural", "epidural", "computed tomography", "magnetic resonance imaging", and "haemorrhagic transformation". Only articles in English were reviewed in detail. The final list of publications was selected by the authors on the basis of relevance to the topic.

Further studies of more patients with serial scanning are needed to better characterise the dynamic nature of perihematomal metabolic changes.¹⁰⁹

Another promising approach is diffusion tensor imaging (figure 6). Diffusion tensor imaging can be used to visualise white matter fibres and map fibre tracts (eg, the corticospinal tract). This technique might be particularly useful to understand the process and potential of motor recovery by assessment of the integrity of the corticospinal tract in the acute, subacute, and chronic stages of intracerebral haemorrhage.¹¹⁰ In patients with intracerebral haemorrhage secondary to cerebral amyloid angiopathy, diffusion tensor imaging shows a characteristic pattern of regional tissue degeneration.¹¹¹

Future approaches to neuroimaging research are likely to be available for clinical studies of haemorrhage and might include high-strength magnets (eg, 8 Tesla) to detect microhaemorrhages and cerebrovascular amyloid, in addition to tissue probes and imaging biomarkers of inflammation, oedema, and excitotoxicity. An important future goal of neuroimaging techniques will include imaging-guided therapy that targets specific stages of injury (eg, blood-brain barrier disruption, oedema, or inflammation).

Conclusions

Neuroimaging sequences have a crucial role in the diagnosis of intracranial haemorrhage, and advances in neuroimaging techniques will continue to provide future insights into the mechanisms of injury. One of the most promising future applications of imaging is to validate markers of increased risk of haemorrhagic transformation in patients with ischaemic stroke and to use this information to guide treatment and develop therapies that reduce risk (eg, drugs that stabilise the blood-brain barrier). An important area for future research is to determine whether neuroimaging findings can be used as a surrogate outcome measure to test acute therapies for primary intraparenchymal haemorrhages. In addition, these imaging techniques have the potential to provide further insights into the timecourse and probable dynamic pathophysiology of injury in patients with intracerebral haemorrhage. New techniques, including magnetic resonance spectroscopy and diffusion tensor imaging, might have important

applications in the understanding of injury due to and recovery from haemorrhage.

Contributors

The authors contributed equally to all parts of this Review.

Acknowledgments

The authors wish to thank Pratik Mukherjee and Geoffrey T Manley, University of California, San Francisco, for figure 6b.

Conflicts of interest

CSK receives funding from the National Institute of Neurological Disorders and Stroke (U54NS057405 and P50 NS44378). MW receives funding from the National Center for Research Resources (KL2 RR024130), GE Healthcare, Philips Medical Systems, and Boston Scientific. MW is a consultant for Paion, Lundbeck, and Concentric. The content of this article is solely the responsibility of the authors and does not necessarily represent the official views of the National Institute of Neurological Disorders and Stroke, the National Center for Research Resources, the National Institutes of Health, and the other sponsors.

References

- Hill MD, Silver FL, Austin PC, Tu JV. Rate of stroke recurrence in patients with primary intracerebral hemorrhage. *Stroke* 2000; **31**: 123–27.
- Broderick J, Connolly S, Feldmann E, et al. Guidelines for the management of spontaneous intracerebral hemorrhage in adults: 2007 update. A guideline from the American Heart Association/American Stroke Association Stroke Council, High Blood Pressure Research Council, and the Quality of Care and Outcomes in Research Interdisciplinary Working Group. *Stroke* 2007; **38**: 2001–23.
- Suarez JI, Tarr RW, Selman WR. Aneurysmal subarachnoid hemorrhage. *N Engl J Med* 2006; **354**: 387–96.
- Osborn AG. Intracranial hemorrhage. *Diagnostic Neuroradiology*. St. Louis: Mosby, 1994: 154–98.
- Parizel PM, Makkat S, Van Miert E, Van Goethem JW, van den Hauwe L, De Schepper AM. Intracranial hemorrhage: principles of CT and MRI interpretation. *Eur Radiol* 2001; **11**: 1770–83.
- Patel MR, Edelman RR, Warach S. Detection of hyperacute primary intraparenchymal hemorrhage by magnetic resonance imaging. *Stroke* 1996; **27**: 2321–24.
- Linfante I, Llinas RH, Caplan LR, Warach S. MRI features of intracerebral hemorrhage within 2 hours from symptom onset. *Stroke* 1999; **30**: 2263–67.
- Schellinger PD, Jansen O, Fiebach JB, Hacke W, Sartor K. A standardized MRI stroke protocol: comparison with CT in hyperacute intracerebral hemorrhage. *Stroke* 1999; **30**: 765–68.
- Alemany Ripoll M, Stenborg A, Sonninen P, Terent A, Raininko R. Detection and appearance of intraparenchymal haematomas of the brain at 1.5 T with spin-echo, FLAIR and GE sequences: poor relationship to the age of the haematoma. *Neuroradiology* 2004; **46**: 435–43.
- Wiesmann M, Mayer TE, Yousry I, Hamann GF, Bruckmann H. Detection of hyperacute parenchymal hemorrhage of the brain using echo-planar T2*-weighted and diffusion-weighted MRI. *Eur Radiol* 2001; **11**: 849–53.
- Lin DD, Filippi CG, Steever AB, Zimmerman RD. Detection of intracranial hemorrhage: comparison between gradient-echo images and b(0) images obtained from diffusion-weighted echo-planar sequences. *AJNR* 2001; **22**: 1275–81.
- Kidwell CS, Chalela JA, Saver JL, et al. Comparison of MRI and CT for detection of acute intracerebral hemorrhage. *JAMA* 2004; **292**: 1823–30.
- Zaheer A, Ozsunar Y, Schaefer PW. Magnetic resonance imaging of cerebral hemorrhagic stroke. *Top Magn Reson Imaging* 2000; **11**: 288–99.
- Wintermark M, Maeder P, Reichhart M, Schnyder P, Bogousslavsky J, Meuli R. MR pattern of hyperacute cerebral hemorrhage. *J Magn Reson Imaging* 2002; **15**: 705–09.
- Woo D, Broderick JP. Spontaneous intracerebral hemorrhage: epidemiology and clinical presentation. *Neurosurg Clin N Am* 2002; **13**: 265–79.
- Lang EW, Ren Ya Z, Preul C, et al. Stroke pattern interpretation: the variability of hypertensive versus amyloid angiopathy hemorrhage. *Cerebrovasc Dis* 2001; **12**: 121–30.

- 17 Fiebach JB, Schellinger PD, Jansen O, et al. CT and diffusion-weighted MR imaging in randomized order: diffusion-weighted imaging results in higher accuracy and lower interrater variability in the diagnosis of hyperacute ischemic stroke. *Stroke* 2002; **33**: 2206–10.
- 18 Chalela JA, Kidwell CS, Nentwich LM, et al. Magnetic resonance imaging and computed tomography in emergency assessment of patients with suspected acute stroke: a prospective comparison. *Lancet* 2007; **369**: 293–98.
- 19 Packard AS, Kase CS, Aly AS, Barest GD. “Computed tomography-negative” intracerebral hemorrhage: case report and implications for management. *Arch Neurol* 2003; **60**: 1156–59.
- 20 Singer OC, Sitzer M, du Mesnil de Rochemont R, Neumann-Haefelin T. Practical limitations of acute stroke MRI due to patient-related problems. *Neurology* 2004; **62**: 1848–49.
- 21 Park J, Hwang YH, Baik SK, Kim YS, Park SH, Hamm IS. Angiographic examination of spontaneous putaminal hemorrhage. *Cerebrovasc Dis* 2007; **24**: 434–38.
- 22 Brott T, Broderick J, Kothari R. Early hemorrhage growth in patients with intracerebral hemorrhage. *Stroke* 1997; **28**: 1–5.
- 23 Broderick JP, Diringer MN, Hill MD, Brun NC, Mayer SA, Steiner T, Skolnick BE, Davis SM. Determinants of intracerebral hemorrhage growth: an exploratory analysis. *Stroke* 2007; **38**: 1072–75.
- 24 Castellanos M, Leira R, Tejada J, Gil-Peralta A, Davalos A, Castillo J. Predictors of good outcome in medium to large spontaneous supratentorial intracerebral haemorrhages. *J Neurol Neurosurg and Psych* 2005; **76**: 691–95.
- 25 Goldstein JN, Fazen LE, Snider R. Contrast extravasation on CT angiography predicts hematoma expansion in intracerebral hemorrhage. *Neuro* 2007; **68**: 889–94.
- 26 Wada R, Aviv RI, Fox AJ, et al. CT angiography “spot sign” predicts hematoma expansion in acute intracerebral hemorrhage. *Stroke* 2007; **38**: 1257–62.
- 27 Kim J, Smith AB, Hemphill JC, et al. Contrast extravasation on multislice CT-angiography and post-contrast CT is an independent predictor of mortality in patients with primary intracerebral hemorrhage. *AJNR* 2007; published online December 7. DOI:10.3174/ajnr.A0859
- 28 Siddique MS, Fernandes HM, Wooldridge TD, Fenwick JD, Slomka P, Mendelow AD. Reversible ischemia around intracerebral hemorrhage: a single-photon emission computerized tomography study. *J Neurosurg* 2002; **96**: 736–41.
- 29 Zazulia AR, Diringer MN, Videen TO, et al. Hypoperfusion without ischemia surrounding acute intracerebral hemorrhage. *J Cereb Blood Flow Metab* 2001; **21**: 804–10.
- 30 Rosand J, Eskey C, Chang Y, Gonzalez RG, Greenberg SM, Koroshetz WJ. Dynamic single-section CT demonstrates reduced cerebral blood flow in acute intracerebral hemorrhage. *Cerebrovasc Dis* 2002; **14**: 214–20.
- 31 Sills C, Villar-Cordova C, Pasteur W, et al. Demonstration of hypoperfusion surrounding intracerebral hemorrhage in humans. *J Stroke Cerebrovasc Dis* 1996; **6**: 17–24.
- 32 Kidwell CS, Saver JL, Mattiello J, et al. Diffusion-perfusion MR evaluation of perihematomal injury in hyperacute intracerebral hemorrhage. *Neurol* 2001; **57**: 1611–17.
- 33 Fainardi E, Borrelli M, Saletti A, et al. Assessment of acute spontaneous intracerebral hematoma by CT perfusion imaging. *J Neuroradiol* 2005; **32**: 333–36.
- 34 Butcher KS, Baird T, MacGregor L, Desmond P, Tress B, Davis S. Perihematomal edema in primary intracerebral hemorrhage is plasma derived. *Stroke* 2004; **35**: 1879–85.
- 35 Herweh C, Juttler E, Schellinger PD, et al. Evidence against a perihemorrhagic penumbra provided by perfusion computed tomography. *Stroke* 2007; published online September 27. DOI:10.1161/STROKEAHA.107.486977
- 36 Forbes KP, Pipe JG, Heiserman JE. Diffusion-weighted imaging provides support for secondary neuronal damage from intraparenchymal hematoma. *Neuroradiol* 2003; **45**: 363–67.
- 37 Pascual AM, Lopez-Mut JV, Benlloch V, Chamorro R, Soler J, Lainez MJ. Perfusion-weighted magnetic resonance imaging in acute intracerebral hemorrhage at baseline and during the 1st and 2nd week: a longitudinal study. *Cerebrovasc Dis* 2007; **23**: 6–13.
- 38 Qureshi AI, Wilson DA, Hanley DF, Traystman RJ. No evidence for an ischemic penumbra in massive experimental intracerebral hemorrhage. *Neurol* 1999; **52**: 266–72.
- 39 Hirano T, Read SJ, Abbott DF, et al. No evidence of hypoxic tissue on ¹⁸F-fluoromisonidazole PET after intracerebral hemorrhage. *Neurol* 1999; **53**: 2179–82.
- 40 Schellinger PD, Fiebach JB, Hoffmann K, et al. Stroke MRI in intracerebral hemorrhage: is there a perihemorrhagic penumbra? *Stroke* 2003; **34**: 1674–79.
- 41 Mayer SA, Lignelli A, Fink ME, et al. Perilesional blood flow and edema formation in acute intracerebral hemorrhage: a SPECT study. *Stroke* 1998; **29**: 1791–98.
- 42 Murakami M, Fujioka S, Oyama T, Kuroda J, Tajiri S, Kuratsu J. Serial changes in the regional cerebral blood flow of patients with hypertensive intracerebral hemorrhage—long-term follow-up SPECT study. *J Neurosurg Sci* 2005; **49**: 117–24.
- 43 Fazekas F, Kleinert R, Roob G, et al. Histopathologic analysis of foci of signal loss on gradient-echo T2*-weighted MR images in patients with spontaneous intracerebral hemorrhage: evidence of microangiopathy-related microbleeds. *AJNR* 1999; **20**: 637–42.
- 44 Kwa VI, Franke CL, Verbeeten B, Stam J. Silent intracerebral microhemorrhages in patients with ischemic stroke. Amsterdam Vascular Medicine Group. *Ann Neurol* 1998; **44**: 372–77.
- 45 Jeerakathil T, Wolf PA, Beiser A, et al. Cerebral microbleeds: prevalence and associations with cardiovascular risk factors in the Framingham Study. *Stroke* 2004; **35**: 1831–35.
- 46 Roob G, Fazekas F. Magnetic resonance imaging of cerebral microbleeds. *Curr Opin Neurol* 2000; **13**: 69–73.
- 47 Greenberg SM, O'Donnell HC, Schaefer PW, Kraft E. MRI detection of new hemorrhages: potential marker of progression in cerebral amyloid angiopathy. *Neurology* 1999; **53**: 1135–38.
- 48 Tanaka A, Ueno Y, Nakayama Y, Takano K, Takebayashi S. Small chronic hemorrhages and ischemic lesions in association with spontaneous intracerebral hematomas. *Stroke* 1999; **30**: 1637–42.
- 49 Kinoshita T, Okudera T, Tamura H, Ogawa T, Hatazawa J. Assessment of lacunar hemorrhage associated with hypertensive stroke by echo-planar gradient-echo T2*-weighted MRI. *Stroke* 2000; **31**: 1646–50.
- 50 Tsushima Y, Tamura T, Unno Y, Kusano S, Endo K. Multifocal low-signal brain lesions on T2*-weighted gradient-echo imaging. *Neuroradiology* 2000; **42**: 499–504.
- 51 Greenberg SM, Briggs ME, Hyman BT, et al. Apolipoprotein E epsilon 4 is associated with the presence and earlier onset of hemorrhage in cerebral amyloid angiopathy. *Stroke* 1996; **27**: 1333–37.
- 52 Tsushima Y, Aoki J, Endo K. Brain microhemorrhages detected on T2*-weighted gradient-echo MR images. *AJNR* 2003; **24**: 88–96.
- 53 Dichgans M, Holtmannspotter M, Herzog J, Peters N, Bergmann M, Youssry TA. Cerebral microbleeds in CADASIL: a gradient-echo magnetic resonance imaging and autopsy study. *Stroke* 2002; **33**: 67–71.
- 54 Gould DB, Phalan FC, van Mil SE, et al. Role of COL4A1 in small-vessel disease and hemorrhagic stroke. *N Engl J Med* 2006; **354**: 1489–96.
- 55 Vahedi K, Boukobza M, Massin P, Gould DB, Tournier-Lasserre E, Bousser MG. Clinical and brain MRI follow-up study of a family with COL4A1 mutation. *Neurology* 2007; **69**: 1564–68.
- 56 Kidwell CS, Saver JL, Villablanca JP, et al. Magnetic resonance imaging detection of microbleeds before thrombolysis: an emerging application. *Stroke* 2002; **33**: 95–98.
- 57 Wong KS, Chan YL, Liu JY, Gao S, Lam WW. Asymptomatic microbleeds as a risk factor for aspirin-associated intracerebral hemorrhages. *Neurology* 2003; **60**: 511–13.
- 58 Chalela JA, Kang DW, Warach S. Multiple cerebral microbleeds: MRI marker of a diffuse hemorrhage-prone state. *J Neuroimaging* 2004; **14**: 54–57.
- 59 Kakuda W, Thijs VN, Lansberg MG, et al. Clinical importance of microbleeds in patients receiving IV thrombolysis. *Neurology* 2005; **65**: 1175–178.
- 60 Fiehler J, Albers GW, Boulanger JM, et al. Bleeding risk analysis in stroke imaging before thrombolysis (BRASIL): pooled analysis of T2*-weighted magnetic resonance imaging data from 570 patients. *Stroke* 2007; **38**: 2738–44.

- 61 Knudsen KA, Rosand J, Karluk D, Greenberg SM. Clinical diagnosis of cerebral amyloid angiopathy: validation of the Boston criteria. *Neurology* 2001; **56**: 537–39.
- 62 Greenberg SM, Eng JA, Ning M, Smith EE, Rosand J. Hemorrhage burden predicts recurrent intracerebral hemorrhage after lobar hemorrhage. *Stroke* 2004; **35**: 1415–20.
- 63 Imaizumi T, Horita Y, Hashimoto Y, Niwa J. Dotlike hemosiderin spots on T2*-weighted magnetic resonance imaging as a predictor of stroke recurrence: a prospective study. *J Neurosurg* 2004; **101**: 915–20.
- 64 Katayama Y, Tsubokawa T, Kinoshita K, Himi K. Intraparenchymal blood-fluid levels in traumatic intracerebral haematomas. *Neuroradiology*. 1992; **34**: 381–83.
- 65 Pflieger MJ, Hardee EP, Contant CF, Jr, Hayman LA. Sensitivity and specificity of fluid-blood levels for coagulopathy in acute intracerebral hematomas. *AJNR* 1994; **15**: 217–23.
- 66 Tong KA, Ashwal S, Holshouser BA, et al. Hemorrhagic shearing lesions in children and adolescents with posttraumatic diffuse axonal injury: improved detection and initial results. *Radiology* 2003; **227**: 332–39.
- 67 McEvoy AW, Kitchen ND, Thomas DG. Intracerebral haemorrhage and drug abuse in young adults. *B J Neurosurg* 2000; **14**: 449–54.
- 68 Tung GA, Julius BD, Rogg JM. MRI of intracerebral hematoma: value of vasogenic edema ratio for predicting the cause. *Neuroradiology* 2003; **45**: 357–62.
- 69 Berger C, Fiorelli M, Steiner T, et al. Hemorrhagic transformation of ischemic brain tissue: asymptomatic or symptomatic? *Stroke* 2001; **32**: 1330–35.
- 70 Nighoghossian N, Hermier M, Berthezene Y. Early diagnosis of hemorrhagic transformation: diffusion/perfusion-weighted MRI versus CT scan. *Cerebrovasc Dis* 2001; **11**: 151–56.
- 71 Arnould MC, Grandin CB, Peeters A, Cosnard G, Duprez TP. Comparison of CT and three MR sequences for detecting and categorizing early (48 hours) hemorrhagic transformation in hyperacute ischemic stroke. *AJNR* 2004; **25**: 939–44.
- 72 Patel SC, Levine SR, Tilley BC, et al. Lack of clinical significance of early ischemic changes on computed tomography in acute stroke. *JAMA* 2001; **286**: 2830–38.
- 73 Hacke W, Kaste M, Fieschi C, et al. Intravenous thrombolysis with recombinant tissue plasminogen activator for acute hemispheric stroke. The European Cooperative Acute Stroke Study (ECASS). *JAMA*. 1995; **274**: 1017–25.
- 74 Larrue V, von Kummer R, del Zoppo G, Bluhmki E. Hemorrhagic transformation in acute ischemic stroke. Potential contributing factors in the European Cooperative Acute Stroke Study. *Stroke* 1997; **28**: 957–60.
- 75 Fiorelli M, Bastianello S, von Kummer R, et al. Hemorrhagic transformation within 36 hours of a cerebral infarct: relationships with early clinical deterioration and 3-month outcome in the European Cooperative Acute Stroke Study I (ECASS I) cohort. *Stroke* 1999; **30**: 2280–84.
- 76 Dzialowski I, Pexman JH, Barber PA, Demchuk AM, Buchan AM, Hill MD. Asymptomatic hemorrhage after thrombolysis may not be benign: prognosis by hemorrhage type in the Canadian alteplase for stroke effectiveness study registry. *Stroke* 2007; **38**: 75–79.
- 77 Lin K, Kazmi KS, Law M, Babb J, Peccherelli N, Pramanik BK. Measuring elevated microvascular permeability and predicting hemorrhagic transformation in acute ischemic stroke using first-pass dynamic perfusion CT imaging. *AJNR* 2007; **28**: 1292–98.
- 78 Latour LL, Kang DW, Ezzeddine MA, Chalela JA, Warach S. Early blood-brain barrier disruption in human focal brain ischemia. *Ann Neurol* 2004; **56**: 468–77.
- 79 Bang OY, Buck BH, Saver JL, et al. Prediction of hemorrhagic transformation after recanalization therapy using T2*-permeability magnetic resonance imaging. *Ann Neurol* 2007; **62**: 170–76.
- 80 Lansberg MG, Thijs VN, Bammer R, et al. Risk factors of symptomatic intracerebral hemorrhage after tPA therapy for acute stroke. *Stroke* 2007; **38**: 2275–78.
- 81 Singer OC, Humpich MC, Fiehler J, et al. Risk for symptomatic intracerebral hemorrhage after thrombolysis assessed by diffusion-weighted magnetic resonance imaging. *Ann Neurol* 2007; published online September 19. DOI:10.1002/ana.21222
- 82 Selim M, Fink JN, Kumar S, et al. Predictors of hemorrhagic transformation after intravenous recombinant tissue plasminogen activator: prognostic value of the initial apparent diffusion coefficient and diffusion-weighted lesion volume. *Stroke* 2002; **33**: 2047–52.
- 83 Stuckey SL, Goh TD, Heffernan T, Rowan D. Hyperintensity in the subarachnoid space on FLAIR MRI. *AJNR* 2007; **189**: 913–21.
- 84 Moustafa RR, Allen CM, Baron JC. Call-Fleming syndrome associated with subarachnoid haemorrhage: three new cases. *J Neurol Neurosurg Psych* 2007; published online December 12. DOI:10.1136/jnnp.2007.134635.
- 85 Wintermark M, Uske A, Chalaron M, et al. Multislice computerized tomography angiography in the evaluation of intracranial aneurysms: a comparison with intra-arterial digital subtraction angiography. *J Neurosurg* 2003; **98**: 828–36.
- 86 Bradley WG, Jr, Schmidt PG. Effect of methemoglobin formation on the MR appearance of subarachnoid hemorrhage. *Radiology* 1985; **156**: 99–103.
- 87 Wahlgren NG, Lindquist C. Haem derivatives in the cerebrospinal fluid after intracranial haemorrhage. *Eur Neurol* 1987; **26**: 216–21.
- 88 Bakshi R, Kamran S, Kinkel PR, et al. Fluid-attenuated inversion-recovery MR imaging in acute and subacute cerebral intraventricular hemorrhage. *AJNR* 1999; **20**: 629–36.
- 89 Atlas SW. MR imaging is highly sensitive for acute subarachnoid hemorrhage...not! *Radiology*. 1993; **186**: 319–22.
- 90 Hajnal JV, Bryant DJ, Kasuboski L, et al. Use of fluid attenuated inversion recovery (FLAIR) pulse sequences in MRI of the brain. *J Comput Assist Tomogr* 1992; **16**: 841–44.
- 91 Noguchi K, Ogawa T, Seto H, et al. Subacute and chronic subarachnoid hemorrhage: diagnosis with fluid-attenuated inversion-recovery MR imaging. *Radiology* 1997; **203**: 257–62.
- 92 Kamran S, Bener AB, Alper D, Bakshi R. Role of fluid-attenuated inversion recovery in the diagnosis of meningitis: comparison with contrast-enhanced magnetic resonance imaging. *J Comput Assist Tomogr* 2004; **28**: 68–72.
- 93 Singh SK, Agris JM, Leeds NE, Ginsberg LE. Intracranial leptomeningeal metastases: comparison of depiction at FLAIR and contrast-enhanced MR imaging. *Radiology* 2000; **17**: 50–53.
- 94 Toyoda K, Ida M, Fukuda K. Fluid-attenuated inversion recovery intraarterial signal: an early sign of hyperacute cerebral ischemia. *AJNR* 2001; **22**: 1021–29.
- 95 Anzai Y, Ishikawa M, Shaw DW, Artru A, Yarnykh V, Maravilla KR. Paramagnetic effect of supplemental oxygen on CSF hyperintensity on fluid-attenuated inversion recovery MR images. *AJNR* 2004; **25**: 274–79.
- 96 Braga FT, da Rocha AJ, Hernandez Filho G, Arikawa RK, Ribeiro IM, Fonseca RB. Relationship between the concentration of supplemental oxygen and signal intensity of CSF depicted by fluid-attenuated inversion recovery imaging. *AJNR* 2003; **24**: 1863–68.
- 97 Mohamed M, Heasley DC, Yagmurlu B, Yousem DM. Fluid-attenuated inversion recovery MR imaging and subarachnoid hemorrhage: not a panacea. *AJNR* 2004; **25**: 545–50.
- 98 Noguchi K, Seto H, Kamisaki Y, Tomizawa G, Toyoshima S, Watanabe N. Comparison of fluid-attenuated inversion-recovery MR imaging with CT in a simulated model of acute subarachnoid hemorrhage. *AJNR* 2000; **21**: 923–27.
- 99 Woodcock RJ, Jr, Short J, Do HM, Jensen ME, Kallmes DF. Imaging of acute subarachnoid hemorrhage with a fluid-attenuated inversion recovery sequence in an animal model: comparison with non-contrast-enhanced CT. *AJNR* 2001; **22**: 1698–703.
- 100 Fiebach JB, Schellinger PD, Geletnek K, Wilde P, Meyer M, Hacke W, Sartor K. MRI in acute subarachnoid haemorrhage; findings with a standardised stroke protocol. *Neuroradiology* 2004; **46**: 44–48.
- 101 Sohn CH, Baik SK, Lee HJ, et al. MR imaging of hyperacute subarachnoid and intraventricular hemorrhage at 3T: a preliminary report of gradient echo T2*-weighted sequences. *AJNR* 2005; **26**: 662–65.
- 102 Duhem R, Vinchon M, Tonnelle V, Soto-Ares G, Leclerc X. [Main temporal aspects of the MRI signal of subdural hematomas and practical contribution to dating head injury]. *Neuro-Chirurgie* 2006; **52**: 93–104.

- 103 Gean AD. Extra-axial collections. *Imaging of Head Trauma*. New York: Raven Press, 1994: 75–145.
- 104 Johnson KA, Gregas M, Becker JA, et al. Imaging of amyloid burden and distribution in cerebral amyloid angiopathy. *Ann Neurol* 2007; **62**: 229–34.
- 105 Kahraman S, Kayali H, Atabey C, Acar F, Gocmen S. The accuracy of near-infrared spectroscopy in detection of subdural and epidural hematomas. *J Trauma* 2006; **61**: 1480–83.
- 106 Kessel B, Jeroukhimov I, Ashkenazi I, et al. Early detection of life-threatening intracranial haemorrhage using a portable near-infrared spectroscopy device. *Injury* 2007; **38**: 1065–68.
- 107 Kobayashi M, Takayama H, Suga S, Mihara B. Longitudinal changes of metabolites in frontal lobes after hemorrhagic stroke of basal ganglia: a proton magnetic resonance spectroscopy study. *Stroke* 2001; **32**: 2237–45.
- 108 Yang DJ, Son BC, Baik HM, Lee SW, Sung JH, Choe BY. Proton magnetic resonance spectroscopic changes of the primary motor cortex and supplementary motor area in hemiparetic patients with corticospinal tract injury due to deep intracerebral hematoma. *J Korean Med Sci* 2004; **19**: 744–49.
- 109 Carhuapoma JR, Wang P, Beauchamp NJ, Hanley DF, Barker PB. Diffusion-perfusion MR evaluation and spectroscopy before and after surgical therapy for intracerebral hemorrhage. *Neurocrit Care* 2005; **2**: 23–27.
- 110 Cho SH, Kim DG, Kim DS, Kim YH, Lee CH, Jang SH. Motor outcome according to the integrity of the corticospinal tract determined by diffusion tensor tractography in the early stage of corona radiata infarct. *Neurosci Lett* 2007; **426**: 123–27.
- 111 Salat DH, Smith EE, Tuch DS, et al. White matter alterations in cerebral amyloid angiopathy measured by diffusion tensor imaging. *Stroke* 2006; **37**: 1759–64.